Applied Energy 195 (2017) 184–195

Contents lists available at ScienceDirect

Applied Energy

journal homepage: www.elsevier.com/locate/apenergy

Reduction of heat pump induced peak electricity use and required generation capacity through thermal energy storage and demand response

Brecht Baeten [a,*], Frederik Rogiers [a], Lieve Helsen [b,c]

[a] KU Leuven Technology campus Diepenbeek, Agoralaan Building B Box 8, B-3590 Diepenbeek, Belgium
[b] KU Leuven, Division Applied Mechanics and Energy Conversion, Department of Mechanical Engineering, KU Leuven, Celestijnenlaan 300 Box 2421, B-3001 Leuven, Belgium
[c] EnergyVille, Thor Park, B-3600 Waterschei, Belgium

HIGHLIGHTS

- A multi-objective MPC strategy for residential heating with heat pumps is presented.
- The simulations employ detailed models for heat pump and thermal energy storage.
- The feedback of individual controllers on the electricity generation is included.
- Results show a significant reduction in required generation capacity is possible.
- Costs carried by the consumer rise when demand response is applied.

ARTICLE INFO

Article history:
Received 13 December 2016
Received in revised form 14 February 2017
Accepted 10 March 2017
Available online 17 March 2017

Keywords:
Demand response
Model predictive control
Heat pump
Thermal energy storage
Peak energy use
Peak generation capacity

ABSTRACT

Shifting residential space heating from the use of gas boilers towards the use of heat pumps is recognized as a method to reduce green house gas emissions and increase energy efficiency and the share of renewable energy sources. Demand response of these systems could aid in reducing peak loads on the electricity grid. Extra flexibility can be added in the form of a thermal energy storage tank. This paper proposes a multi-objective model predictive control strategy for such a system, which takes into account the users energy cost, the environmental impact of energy use and the impact of expanding the electricity generation capacity. This control strategy is used in a case study inspired by the Belgian electricity generation park with 500,000 heat pumps to investigate the effect of the size of a space heating storage tank on consumer cost, energy use and required electricity generation capacity. Results indicate that the proposed demand response strategy reduces the required peak load capacity substantially with only a small increase in costs for the consumer. When adding a large hot water storage tank, the required additional capacity is nearly eliminated. Independently of the required capacity, the controller shifts energy use from peak to base generating plants. Increasing the storage tank size increases the amount of energy that is shifted. However, when demand response is applied by using a space heating storage tank, the costs for the consumer always increase relative to the case without demand response or storage tank. If demand response is desired by the grid operator, heat pump owners should be encouraged to participate by remunerating them for their additional expenses.

1. Introduction

Global warming caused by the emission of greenhouse gases is expected to have irreversible effects on the environment and human society in the near future unless emissions are decreased [1]. The European Union has set targets for increasing renewable energy use, increasing energy efficiency and reducing greenhouse gas emissions which aid in tackling global warming [2,3].

Electrifying residential heating loads through the use of heat pumps, can contribute to all goals set above. Moreover, this increases the viability of large scale deployment of non-dispatchable renewable energy conversion by increasing the load factor [4–6]. However, the introduction of large numbers of heat pumps in the electricity grid could disrupt the load diversity.

* Corresponding author.
E-mail address: brecht.baeten@kuleuven.be (B. Baeten).

http://dx.doi.org/10.1016/j.apenergy.2017.03.055
0306-2619/

In an electricity grid, load diversity lowers the required generation capacity [7]. Unfortunately, space heating is a highly simultaneous load as it is predominantly ambient temperature dependent. When heat pumps are deployed for space heating on a large scale, large peak loads are expected in winter times [8]. Demand response (DR) is referred to in the literature as technologies or programs that concentrate on shifting energy use to help balance supply and demand [9]. Several authors have identified DR as a means to reduce peak loads generated by heat pump operation [8,10,11]. At times of abundant electricity generated from renewable sources, heat generated by a heat pump can be stored in the structure of the heated building or in a thermal energy storage tank. During a subsequent period of large electricity demand, the heat production of the heat pump can be decreased while releasing the stored thermal energy. This way the peak loads in the electricity grid are decreased while the thermal comfort of the building inhabitants is maintained provided the system is well-controlled. By using a hot water storage tank as thermal energy buffer, the amount of energy which can be stored is increased, thus increasing system flexibility.

Several studies investigate the potential of residential DR with heat pumps. Kreuder and Spataru [12] used a simplified model of heat pump space heating for residential buildings to investigate the effect of demand response on the peak load at household level and electricity generation level. They assumed a DR algorithm which alters the heat pump load to have a constant daily demand profile in each household. Without demand response, the heat pumps cause an increase in peak load of about 2500 W at household level. By introducing a DR method, this peak load is decreased by about 700 W per household. In the model, they calculated the heating loads and heat pump efficiency based on the daily average temperature. Furthermore, effects of part load on heat pump efficiency were neglected. These model simplifications could have a large effect on the results as daily temperature variations significantly affect the heat pump load. Vanhoudt et al. [8] experimentally investigated the effect of an actively controlled heat pump on the buildings energy demand profile. They found that their multi-agent market-based control algorithm decreases the peak load but does not decrease the consumption of fossil-based electricity. The combination of heat pumps and a hot water storage tank for space heating was investigated by Arteconi et al. [13]. They show that even without a storage tank, when sufficient thermal mass is present in the emission system, the heat pump can be turned off during a 3 h peak period without affecting thermal comfort. Arteconi et al. [11] also investigated the effect of the number of DR participants on the total operational costs of electricity generation. In that study, DR is supplied by space heating and DHW production using a domestic hot water tank, no space heating storage tank is considered. In several scenarios of the future Belgian electricity grid they show that with more DR penetration the operational costs decrease but the savings per customer also decrease. As the DR penetration increases the peak residual demand also decreases. However, it remains well above the fixed peak residual demand. The peak demand decrease is driven by the higher energy costs assigned to high demand by a merit order model. Patteeuw et al. [14] computed the cost of a reduction in CO_2 emissions through DR and the use of heat pumps in residential buildings on a large scale. They found that DR reduces the cost although there is a large spread in costs depending on the building insulation level and the heating system. Hedegaard et al. [15] discuss the investment in storage tanks used for space heating with heat pumps in a DR context and compare it with using the building thermal mass to offer flexibility to the electricity generation park. Using simplified models for building and storage tank, they conclude the fuel savings cost is higher for the cases with storage tank than with passive thermal energy storage. However, in the case of passive thermal energy storage the building temperature is allowed to fluctuate in a temperature band around the reference temperature. This implies that there are times the temperature is below the reference temperature meaning the thermal comfort of the building inhabitants is decreased. This difference in thermal comfort results in an unfair comparison between cases.

The afore mentioned studies employ optimal control problems (OCP) with either perfectly stratified or perfectly mixed models to represent the dynamics of hot water storage tanks. However, when using a hot water storage tank for space heating in a demand response context, the effective storage capacity is highly dependent on the degree of stratification inside the tank [16]. The use of simplified models to represent the storage tank behavior thus may over- or underestimate the energy retrievable from the storage tank and the power at which it can be retrieved. On the other hand, the solution of an optimization problem with an accurately modeled hot water storage tank is too time consuming when results on a yearly time scale are required. To resolve this problem a moving horizon optimal control or model predictive control (MPC) simulation can be used. In an MPC simulation a simplified OCP is used to generate control signals for a simulation with a detailed model, known as the system emulator.

In the literature, several authors use MPC or other advanced control strategies to investigate the operation of thermal energy storage in an energy system [17–23]. Bianchini et al. [17] present an MPC algorithm for a large multi-zone building heated by a heat pump. They considered a scenario where an aggregator proposes DR requests, in the form of a price-volume signal, to the building management system. The building owner is rewarded if the requests are fulfilled. Results indicate good thermal comfort while addressing the DR request. However, the effects on the electricity generation were not investigated. Another MPC algorithm which minimizes the cooling costs of a large building based on the day-ahead electricity price is proposed by Zhao et al. [18]. They conclude that using combined cooling and power generation can reduce the buildings primary energy use and CO_2 emissions. Adding a 125 m^3 chilled water energy storage further enables savings in the building energy cost. However, these results are only valid when the penetration of such buildings in the electricity market is low, as no feedback effects are taken into account. Dahl Knudsen and Petersen [19] present an MPC controller which minimizes electricity costs or CO_2 emissions for electric space heating. Depending on the controller settings lower emissions or lower costs compared to a PID control can be obtained. However, the presented control strategies neglect the feedback effects of the demand side changes on the electricity generation side which can be significant [24].

Schibuola et al. [20] investigated several price signal based control strategies for maximizing self consumption in an apartment building. Here, a decrease of imported and exported energy of up to 11% and 21% respectively is seen. Dar et al. [21] found that with different rule based control strategies, self consumption or the energy bill of a net-zero energy building can respectively increase by 40% and decrease by 19%. However, both values are obtained with mutually exclusive control strategies and effects on the electricity generation side are not taken into account.

Furthermore, often price signals are used to represent the electricity generation side. When DR is widespread, the feedback of the individual controllers on the electricity generation must be taken into account [24].

When DR is applied on a large scale, individual controllers impact loading and even commitment of electricity generation units, hereby altering the generation mix. Existing studies on building-level MPC with DR objectives do not take these effects into account. Often price signals are used to represent the

electricity generation side. This approach neglects the feedback of DR on the supply side which actually is its prime objective [24].

This work aims at investigating the effects of a large-scale introduction of actively controlled heat pumps and hot water storage tanks used as space heating energy buffer, incorporating feedback of these systems on the electricity generation. A local model predictive control strategy for residential space heating with heat pump and thermal energy storage is presented. The control strategy is designed to trade-off local costs with system-wide electricity generation environmental impact or required generation capacity. A moving horizon optimal control simulation using a detailed, validated hot water storage tank model is set up. In a case study inspired by the Belgian electricity system with the assumption of a large number of installed heat pumps, the effects of the space heating hot water storage tank size on the system load duration diagrams and the consumer costs are investigated for different control settings.

The remainder of this paper is structured as follows: in Section 2, the system emulation model and simplifications used in the optimal control model are presented. Section 3 describes the overall control approach and the control parameters which influence the trade-offs. Next, in Section 4, the effects of the control parameters on the energy use and required generation capacity are investigated. Finally, the effect of a hot water storage tank as space heating energy buffer is discussed. In Section 5, concluding remarks are formulated.

2. System model

This section describes the system under consideration and its mathematical model. The system consists of a set of similar residential buildings with an underfloor heating system to which heat is supplied by an air to water heat pump. The heat pump uses electricity produced by different renewable and classic power plants. At the building level thermal energy storage capacity is available through the building thermal mass, the underfloor heating, a domestic hot water storage tank and a space heating buffer tank (Fig. 1).

An emulator for the building and heating system is created using the Modelica physical modeling language [25]. In the emulator the governing equations are solved numerically using a variable time step differential-algebraic equation solver implemented in Dymola 2016.

To control the system, an MPC strategy is employed. MPC uses a system model to compute control signals which minimize an objective function. From a given state of the system, an OCP is solved and only the first part of the resulting control signals is applied. Afterwards, the system evolves to a new state and the process is repeated [26–28].

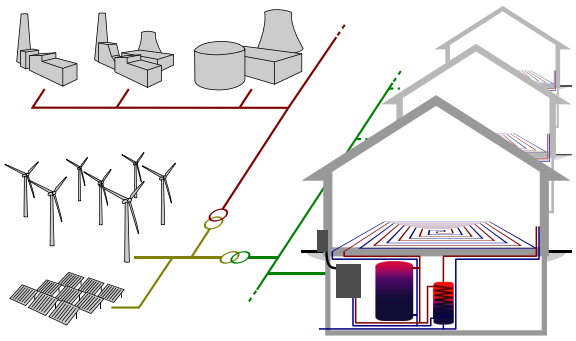

Fig. 1. Schematic representation of the system under consideration, including a set of buildings heated by a heat pump with a hot water storage tank used for space heating and a domestic hot water tank. The electricity production park consists of renewable based and classic electricity generation plants.

The current study applies an MPC control strategy to the system emulator. Every hour, values for the required control signals are computed through the solution of an OCP over a 4 day control horizon. The optimal control problem consists of a simplified model of the system, constraints limiting the allowable operating range and an objective function which is minimized by altering the control signals. The optimal control signals are applied to the system emulator which calculates the system behavior for the next hour. Then, the states of the optimal control problem variables are estimated from the emulator results. Hereafter, the optimal control problem is updated with new initial states and boundaries and the process is repeated. This strategy is sometimes referred to as moving horizon optimal control.

In the following subsections the emulator and controller model for each subsystem are described. As a case study, parameter values derived from the Belgian housing stock and electricity generation park are used. The results presented are thus to be seen within the context of the Belgian electricity system. Nevertheless, the presented multi-objective control strategy can be used independently of the presented case.

2.1. Building

In this paper the set of buildings under consideration is modeled by scaling the results of a single building simulation [29]. This simplification assumes the averaged behavior of the building set is equal to the behavior of the average building, including average user behavior. This assumption is based on the simultaneity of the space heating requirement for all buildings. As heat pumps currently available on the market operate more efficiently in part load operation, this assumption is further justified.

The building under consideration is a new built, detached single family home, insulated according to current Flemish building performance legislation, built with massive construction elements, as is common in Belgium [30]. The building is assumed to have an underfloor emission system which covers the entire ground floor area. Key parameters for the building are presented in Table 1.

In Fig. 2, a simplified model of the building under consideration is presented as an RC-network. This building model is used in the emulator as well as the optimal control problem. The model was extended from [31] to include a basement which functions as technical room where the heating system, including space heating storage tank and domestic hot water tank, are set up. The building interior air (in), internal walls (wi) and furniture, external walls (we), floor (fl) and technical room (tr) temperatures are chosen as state variables. Heat losses from the building are transferred to the ambient air (amb) by transmission and ventilation, and to the ground (gnd), which is assumed to be at a constant temperature. As the floor and all walls are assumed to be built using heavy-weight materials, the floor and external walls thermal resistance is split into parts ($R_{w1} - R_{w2}$ and $R_{f1} - R_{f2}$) on either side of a lumped thermal capacity. The ventilation heat loss is modeled as a thermal resistance (R_{ve}).

Solar and internal gains are modeled as heat flows to all thermal capacities. The solar gains are calculated as a fraction of maximum

Table 1
Key parameters for the building under consideration.

Volume (m^3)	741
Ground floor area (m^2)	132
External surface area (m^2)	530
Total window area (m^2)	44
Average insulation value (W/m^2 K)	0.44

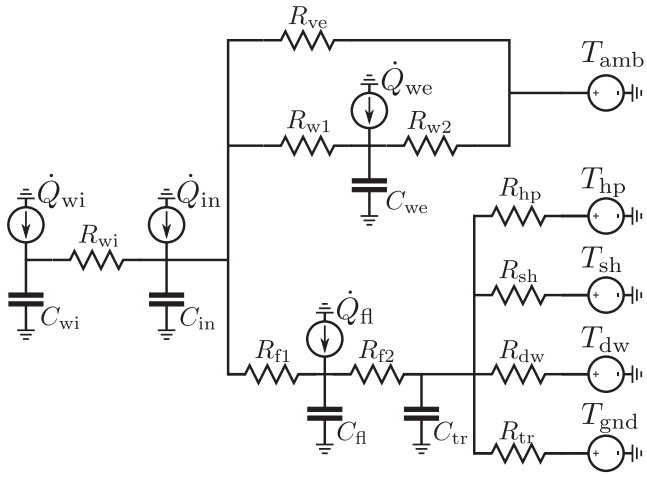

Fig. 2. A detached house with underfloor heating including basement acting as technical room, modeled as an RC-network.

solar gains, determined by the shading position, and distributed over the internal air, internal walls, external walls and floor according to fixed distribution factors [32]. Internal gains are supplied to the interior air temperature.

The heating system is assumed to be located in the technical room (tr) of the building. All parts of the heating system are assumed to have linear heat losses to the technical room. These heat losses can be represented as thermal resistances for the heat pump (hp), space heating storage tank (sh) and domestic hot water storage tank (dw).

From this schematic presentation, differential equations governing the behavior of the system can be derived which are used in the system emulator. In the OCP these equations are discretized with respect to time using a 2nd order collocation scheme and considered as equality constraints (see Appendix A.1).

2.2. Heating system

In Fig. 3 the heating system consisting of heat pump, space heating storage tank, domestic hot water storage tank and electric domestic water heater is presented schematically. In the system under consideration, an air source heat pump is used to supply heat to a space heating storage tank, to the building heat emission system or to the domestic hot water tank. The heat pump and space heating storage tank are connected in parallel to the heat emission system and can be used independently to supply heat to the building. In the present study, cooling of the building is not considered. However, the methodology can be easily extended to include cooling.

In the system emulator, the condenser of a modulating air to water heat pump, with 7.0 kW rated heating capacity, is modeled as a heating element in the hydronic circuit. The heating capacity ($\dot{Q}$) and required power input (P) are modeled using performance maps obtained from manufacturer data. The performance maps relate the heating capacity and the required power to the ambient air temperature, the leaving water temperature and the compressor modulation. The leaving water temperature can be set at three different temperature levels, 35 °C, 45 °C and 55 °C designated low (lt), medium (mt) and high (ht) temperature respectively. The compressor is assumed to modulate continuously from 0% to 100%.

In the optimal control problem, the power required by the heat pump operating at a temperature level is modeled to be quadratically dependent on the heat transferred at the condenser. For each leaving water temperature level, the polynomial coefficients were fit for different ambient temperatures creating a model which is dependent on the leaving water temperature, ambient temperature and modulation. Examples of the fitted data are presented in Fig. 4. This procedure leads to a small heat pump model mismatch between the emulator and the controller. For each temperature level, an inequality constraint is required to maintain convexity of the resulting optimization problem. As additional power use will always result in higher costs this constraint will however always be active.

$$
\begin{aligned}
P_{\mathrm{hp,lt}} &\geqslant \zeta_{\mathrm{l,lt}}(T_{\mathrm{amb}})\dot{Q}_{\mathrm{hp,lt}} + \zeta_{\mathrm{q,lt}}(T_{\mathrm{amb}})\dot{Q}^2_{\mathrm{hp,lt}} \\
P_{\mathrm{hp,mt}} &\geqslant \zeta_{\mathrm{l,mt}}(T_{\mathrm{amb}})\dot{Q}_{\mathrm{hp,mt}} + \zeta_{\mathrm{q,mt}}(T_{\mathrm{amb}})\dot{Q}^2_{\mathrm{hp,mt}} \\
P_{\mathrm{hp,ht}} &\geqslant \zeta_{\mathrm{l,ht}}(T_{\mathrm{amb}})\dot{Q}_{\mathrm{hp,ht}} + \zeta_{\mathrm{q,ht}}(T_{\mathrm{amb}})\dot{Q}^2_{\mathrm{hp,ht}}
\end{aligned} \tag{1}
$$

As the maximum heat pump capacity occurs at 100% modulation, it is only ambient temperature dependent. Thus for the maximum condenser heat flow rate, the manufacturer data are linearly interpolated in the optimal control formulation.

To avoid integers in the optimization problem, the heat pump is allowed to operate at the different leaving water temperatures simultaneously. As this is not possible in reality or in the system emulator, after the optimization, a post processing step reorders the condenser heat flow rates so they occur sequentially within a single control time step while ensuring equal energy transfers at each leaving water temperature level.

The space heating storage tank is assumed to be a vertical cylindrical tank with rounded heads as is available on the market. Several storage tank volumes are simulated by changing the storage diameter while keeping the height fixed at 2 m. The tank is insulated using 20 cm flexible poly-urethane foam with a thermal conductivity of 0.04 W/m K. Fittings attached to the storage tank and penetrating through the insulation are assumed to increase

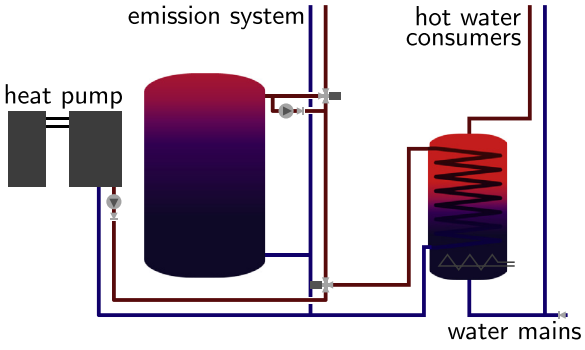

Fig. 3. Diagram of the heating system including a space heating energy storage tank besides the heat pump, domestic hot water storage tank and electric domestic water heater.

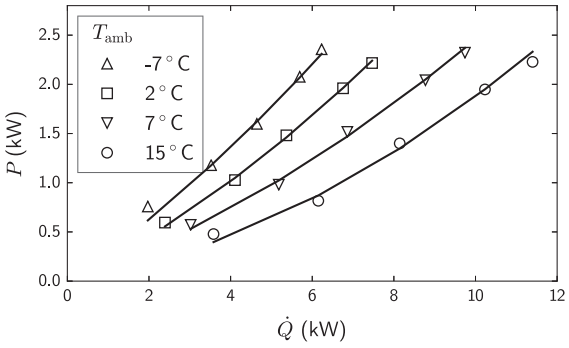

Fig. 4. Example of the heat pump performance data and quadratic curve fit as used in the optimal control problem for the low leaving water temperature level.

heat losses and are modeled with a heat transfer rate of 0.16 W/K. The space heating storage tank is charged and discharged through direct inflow ports positioned horizontally and located at a distance of 0.04 m from the top and bottom. When the monthly average ambient temperature rises above 13 °C, the space heating requirement is very small. The space heating storage tank is then disconnected from the heating system to reduce heat losses. If during this period space heating is required, it is directly supplied by the heat pump.

Domestic hot water is supplied to the building occupants from a 0.2 m^3 domestic hot water storage tank. The domestic hot water tank is charged by the heat pump through an immersed coil heat exchanger spanning the entire storage tank height. An auxiliary immersed resistance heater, located at the bottom of the tank, can be used to further heat the tank up to 80 °C, designated the very high temperature level (vht). As a result of the charging methods, the domestic hot water tank is mixed during charging, so afterwards the storage tank temperature is nearly uniform. To ensure the building users domestic hot water comfort, the storage tank is controlled to be at a temperature of 50 °C every morning at 7 h and to be at 60 °C every evening at 20 h. A high temperature is set every day to avoid legionella contamination as suggested by Vlieger et al. [33]. During a 4 h period after the high temperature set point no storage charging is allowed as domestic hot water draws are assumed to occur in this period. During the morning period 0.09 m^3 and during the evening period 0.15 m^3 water at 45 °C is used every day. When the water in the storage tank is at a higher temperature, a thermostatic mixing valve mixes the water from the storage with cold water from the water mains.

In the emulator, both storage tanks are modeled using a 1D finite volume discretization with 50 layers. An energy balance is formulated for each layer and mixing and buoyancy of the jets entering the storage tanks are modeled in accordance with the method suggested by Baeten et al. [16]. In the OCP the space heating storage tank is modeled as a perfectly stratified storage tank. This results in a constraint limiting the maximum energy flow rate which can flow in or out of the storage tank as stated by Baeten et al. [34]. As water is supplied at a constant temperature and the return water temperature from the emission system will not vary much, ideal stratification is a realistic assumption. The domestic hot water storage tank is modeled in the OCP as being charged perfectly mixed, and discharged perfectly stratified as proposed by Baeten et al. [35]. Mixed charging implies a reduction in power supplied by the heat pump as the temperature of the tank rises. Furthermore, the heat pump cannot deliver any heat to the domestic hot water storage tank when it is heated by the auxiliary heater above the maximum heat pump leaving water temperature. To model this in the optimal control problem, the domestic hot water tank is split in a low, medium, high and very high temperature part which can only be used in sequence as described by Patteeuw and Helsen [36]. The discharging occurs using direct inflow ports of water from the mains and will thus result in stratification of the storage tank.

2.3. Electricity generation

The electricity use of the heat pumps and auxiliary water heaters in the building set is added to the fixed demand in the electricity grid. This total electricity demand needs to be supplied by the available electricity generation plants. The electricity generation park is simplified by dividing it in four categories: Wind generation, photo-voltaic (PV) generation, base load generation and peak load generation plants. At all times the sum of outputs of each part of the electricity generation park must equal the total electricity demand. In this approach, losses in the electricity grid are neglected. Wind, PV and base load generation are assumed to have a limited, fixed capacity. The capacity of all peak load generation plants is assumed large enough. The required peak load capacity is an output of the simulations. To schedule the electricity generation, a merit order model is used as suggested by Patteeuw et al. [24].

The available capacity of wind and PV generation is obtained by upscaling measured power generation data for the Belgian electricity grid in the year 2013 [37]. The capacities are scaled up to 4.08 GW wind power and 5.75 GW PV power, chosen based on the Europe 2030 goals for increasing renewable energy in Belgium [2]. The ratio between wind capacity and PV capacity is equal to the current capacity ratio in Belgium. No distinction is made between on- and offshore wind power. As producing electricity using these renewable technologies releases very little greenhouse gases into the atmosphere, e.g. emissions related to maintenance, they are scheduled first. In this paper the total load minus the available renewable based production is called the residual load. When the renewable sources can generate more than the total electricity demand, residual load is zero and renewable production will be curtailed. When the residual load is larger than zero, it must be supplied by base and peak load power plants. Part of this residual load originates from the fixed load in the electricity grid and thus is also fixed. This part is designated the fixed residual load.

A fixed capacity of low greenhouse gas emission power plants (e.g. nuclear power plants and combined cycle gas turbines) is assumed to be available in the electricity production park. These plants are designated as base load plants and are scheduled second. Throughout this paper a base load generation capacity of 10,000 MW is assumed. This amount is derived from the present relative nuclear and combined cycle gas turbine capacity in Belgium.

Due to technical constraints in the assumed base load power plants, the base load generation has a limited ramping rate. When the available renewable capacity increases, the variations in the residual load increase accordingly. When the residual load suddenly drops below the base load capacity, for instance due to rapidly changing weather conditions, base load power plants may not be able to follow the residual load. They need to anticipate these changes and gradually lower their output in advance. In this study a maximum ramping rate for the entire base load fleet of 10 MW/min is assumed.

The difference between the residual load and the base load plant generation is supplied by peak load power plants (assumed to be open cycle gas turbines). The capacity of the peak load generation plants is not fixed in advance. The required peak load generating capacity is determined by simulation. However, to limit peaks in residual power, an additional cost is added when the residual load is higher than a preset threshold. The determination of this parameter is described in Section 3.

The above assumptions lead to an enhanced merit order model for the electricity generation park, taking maximum base load ramping into account, but neglecting start-up, shut-down, and part load running costs.

In this paper the required energy, generation capacity and consumer heating cost are compared for different systems and control parameters. To compute the consumer cost a day-night time-of-use electricity tariff, as is common in Belgium, is used with an electricity price of 0.25 EUR/kW h during weekdays from 7 h to 22 h and 0.22 EUR/kW h otherwise.

3. Control approach

A direct collocation optimal control problem with a time step of 1 h is formulated. The model equations of the system presented above are discretized and implemented as equality constraints.

For the hot water storage tanks additional constraints are implemented to specify whether the storage behaves stratified or mixed [35]. The complete optimal control formulation is presented in Appendix A.

Different control objectives can be defined. Firstly, from the individual consumer viewpoint, a consumer wants to minimize his own cost for providing thermal comfort and domestic hot water. This can be attained by minimizing the individual cost of energy over the control horizon, stated that thermal comfort is maintained. In the present MPC formulation, a large cost for discomfort is added to the objective function thus treating thermal comfort as a soft constraint:

$$\text{minimize} \quad \sum_{i=\text{time}} p^i_{\text{el}}(P^i_{\text{hp}} + P^i_{\text{aux}})\Delta t + \sum_{i=\text{time}} \text{discomfort costs}^i \tag{2}$$

With p^i_{el} the electricity price at time step i and P^i_{hp} and P^i_{aux} the heat pump power and auxiliary heater power respectively. In this study, the discomfort costs are quantified by multiplying the deviation of the operative building temperature outside set comfort temperature boundaries with a discomfort cost p_d (A.13) where the operative building temperature is calculated according to (A.12).

Secondly, an environmental impact of energy use viewpoint can be considered, where the environmental impact of the used energy is minimized. As the impact differs for each generation plant, the optimization attempts to run the most environmentally friendly plant as much as possible. The objective function is then written as:

$$\text{minimize} \quad \sum_{i=\text{time}} \sum_{j=\text{sup}} p_{\text{impact,j}} P^i_j \Delta t + \sum_{i=\text{time}} \text{discomfort costs}^i \tag{3}$$

With $j = \text{sup}$ an index which runs over all power plants, $p_{\text{impact,j}}$ the marginal impact of generating electricity by plant j and P^i_j, the power generated by plant j in time step i.

In this paper the impacts of power generation for the different plants are chosen as the single score impact for energy generated at rooftop pv, on- and offshore wind, nuclear, combined cycle natural gas and open cycle gas turbine power plants derived from the Ecoinvent database [38].

Finally, one must remark that not only energy use is important when considering the environmental impact of electricity generation. For many power plants, a large amount of emissions are associated with the construction and decommissioning of the plant itself. The costs or emissions assigned to generation capacity are difficult to implement in a moving horizon optimal control approach as the maximum load will occur only in a few optimization horizons. To handle this problem, an overload threshold ($P^{\max}_{\text{overload}}$) is defined. When the residual power generation rises above the overload threshold, an additional cost is assigned to the square of the overload power:

$$\text{minimize} \quad \sum_{i=\text{time}} p_{\text{impact, cap}} \left(P^i_{\text{overload}}\right)^2 \Delta t + \sum_{i=\text{time}} \text{discomfort costs}^i \tag{4}$$
$$\text{subject to} \quad P^i_{\text{overload}} \geqslant P^i_{\text{residual}} - P^{\max}_{\text{overload}}$$

As this is an approximation to include costs for installed capacity in the objective function, the price of capacity assigned here, $p_{\text{impact, cap}}$, has little physical meaning. In this study, it is chosen such that the impact of an overload situation, if it occurs, is substantially larger than the impact of generating electricity at a power just below the overload threshold.

In the present paper, the three viewpoints, consumer cost, energy impact and capacity impact, are merged in a single multi-objective function. To include the energy impact in the consumer cost function, a weighting factor for the environmental impact of energy (w_{EIE}) is introduced which scales the environmental impact of electricity generation to a cost for the consumer. If this factor is small, the controller will disregard the impact of the generated electricity, if it is large, the controller will attempt to minimize the impact. The capacity impact viewpoint can simply be added to the cost function. To alter controller behavior, to attempt to minimize the required capacity or not, the overload threshold is changed. A capacity limiting factor (l_{cap}) is introduced, which relates the overload threshold to the maximum fixed residual load:

$$P^{\max}_{\text{overload}} = l_{\text{cap}} P^{\max}_{\text{residual,fixed}} \tag{5}$$

When the capacity control factor is much larger than 1, overload situations are not recognized by the controller, and load peaks are not avoided. When l_{cap} is near 1 or even below 1, the controller attempts to keep the residual load below the threshold unless thermal comfort is jeopardized.

Combining the above objective functions and definitions, the total objective function is written as:

$$\begin{aligned}\text{minimize} \quad & \sum_{i=\text{time}} p^i_{\text{el}}(P^i_{\text{hp}} + P^i_{\text{aux}})\Delta t + \sum_{i=\text{time}} \sum_{j=\text{sup}} w_{\text{EIE}}\, p_{\text{impact,j}} P^i_j \Delta t \\ & + \sum_{i=\text{time}} p_{\text{impact, cap}} \left(P^i_{\text{overload}}\right)^2 \Delta t + \sum_{i=\text{time}} \text{discomfort costs}^i \\ \text{subject to} \quad & P^i_{\text{overload}} \geqslant P^i_{\text{residual}} - l_{\text{cap}} P^{\max}_{\text{residual,fixed}}\end{aligned} \tag{6}$$

The resulting optimal control problem is a convex quadratically constrained problem with a quadratic objective function and is solved with IBM ILOG CPLEX.

The results of different settings of the two controller parameters (w_{EIE} and l_{cap}) are analyzed in a parametric study with different space heating storage tank sizes. MPC simulations spanning a single year are executed for w_{EIE} equal to 10^{-2}, 10^0 and 10^2 and l_{cap} equal to 1.10, 1.00 and 0.95. The case with $w_{\text{EIE}} = 10^{-2}$ and $l_{\text{cap}} = 1.10$ represents no DR, where every consumer minimizes his own energy bill. With these settings, there is no incentive to lower the electricity use at times of high wholesale market prices or when system reliability is jeopardized. In all other cases DR is present to some degree. To investigate the effects of adding extra storage capacity at the demand side, results are computed for a heating system without space heating storage tank, with a 1 m^3, 2 m^3, and a 4 m^3 storage tank.

During all simulations perfect weather predictions and predictions of available renewable sources are assumed. Furthermore, a perfect estimation of the building states is assumed which is possible as the building model in the optimal control formulation is the same as in the system emulator. The states of the storage tanks are also derived directly from the actual average storage tank temperature as calculated by the system emulator.

4. Results and discussion

In this section the results of the described case study are presented. When comparing different systems or control strategies, it is important that thermal comfort is comparable in all cases. In the present study, the thermal comfort requirements were met almost always. Building operative temperatures never drop below the specified lower comfort limit of 20 °C and the demanded domestic hot water is always delivered. Only during a brief period in summer, the operative temperature rises above the maximum allowed operative temperature of 24 °C. As the building does not include an active cooling system, this is unavoidable. This summer overheating results in a discomfort of around 200 K h for all simulated cases, representing a temperature of 1 K above the maximum value for less than 10 days per year. As this discomfort is comparable in all cases, a fair comparison between cases is made.

In the following subsections different aspects of the results are highlighted. First, the general behavior of the control strategy is illustrated. Next, the effect of different control parameter settings on the required peak generating capacity is discussed. Afterwards, the effect on energy use is presented. Finally, the associated costs for the consumer are compared.

4.1. General control behavior

The effect of adding a space heating storage tank on the residual peak load period is illustrated in Figs. 5 and 6. In Fig. 5 time series of the fixed residual load, heat pump power and auxiliary heater power for a system without storage tank and with a 4 m^3 space heating buffer are compared for a 7 day period. In Fig. 6 the corresponding building and storage tank temperatures are presented. In the presented figures the control settings are $w_{EIE} = 10^2$ and $l_{cap} = 0.95$.

When no space heating buffer is present, only the floor will serve as thermal energy storage (Figs. 5a and Fig. 6a). However, due to the limits on indoor operative temperature, the amount of energy that can be stored, and subsequently the peak load period that can be bridged, is limited. The 4 m^3 storage tank allows the heat pump to be switched off during the time of high fixed residual load without a reduction in thermal comfort for the building occupants (Figs. 5b and 6b). Remarkable is that the storage tank was charged almost 5 days prior to discharge during a period of very low loads. In the period between charge and discharge only the heat losses of the storage tank are being compensated by the heat pump leading to only a small additional heat pump load. Furthermore, it can be seen in Fig. 5 that when a storage tank is used, a small increase in production from base load plants is possible through the increased heat pump operation in periods of low fixed residual demand.

In Fig. 7 the residual load duration diagrams with different storage sizes are presented for the same control settings as above. In addition, the fixed residual load and the residual load without DR are shown. The load without DR is computed with the control settings at $w_{EIE} = 10^{-2}$ and $l_{cap} = 1.10$. With these control settings consumers minimize their local cost, without concerns about the electricity generation efficiency or renewable sources share. Furthermore, with the high capacity control limit, peak loads are disregarded by the control strategy. Differences between different storage tank sizes are difficult to observe in the full load duration diagram. However, the difference with the case without DR is clear. Even without additional storage capacity DR decreases energy use at high loads (which occur during less than 2000 h per year) and increases energy use at lower loads.

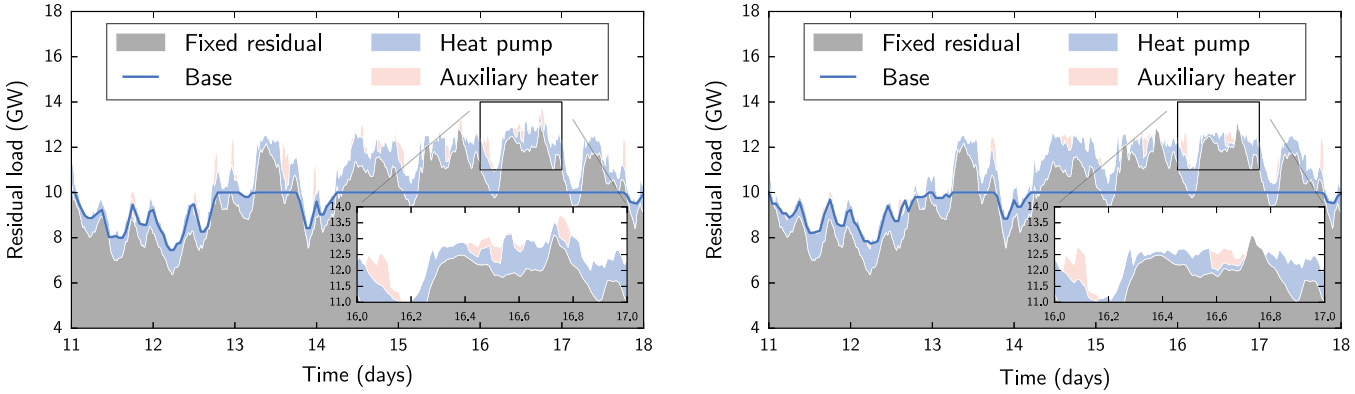

(a) no space heating storage tank (b) 4 m^3 space heating storage tank

Fig. 5. Time series of the residual load during the winter peak period. The residual load is split up into the fixed residual load, the part caused by the heat pump electricity use and the part caused by the auxiliary heater electricity use. The power delivered by base load plants is also presented. On the left no space heating storage tank is present in the buildings. On the right a 4 m^3 hot water storage tank is used to buffer space heating loads. For both results the environmental impact of energy use weight setting is $w_{EIE} = 10^2$ and the capacity limit setting is $l_{cap} = 0.95$.

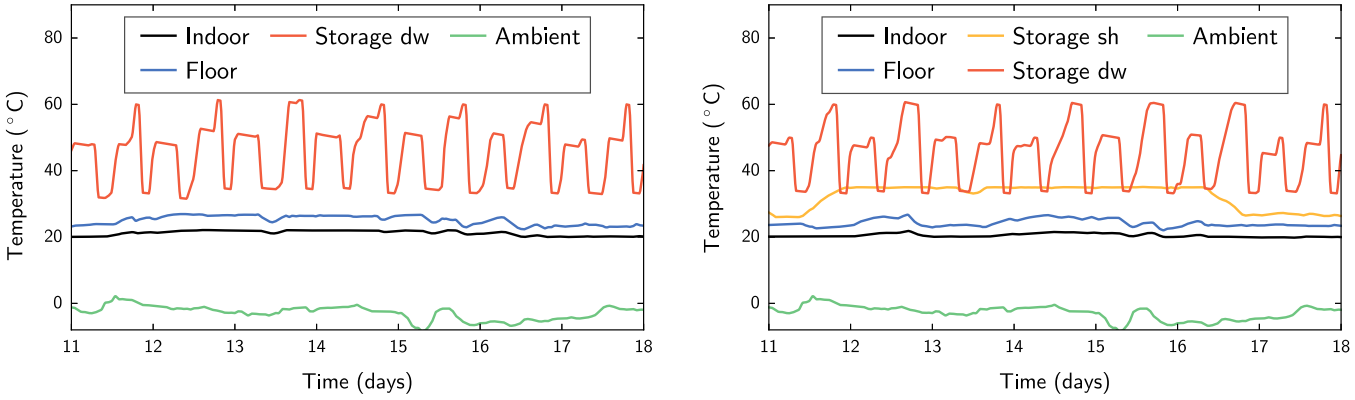

(a) no space heating storage tank (b) 4 m^3 space heating storage tank

Fig. 6. Time series of the most important building and heating system temperatures during the winter peak period. On the left no space heating storage tank is present in the buildings. On the right a 4 m^3 hot water storage tank is used to buffer space heating loads. For both results the energy control setting is $w_{EIE} = 10^2$ and the capacity control setting is $l_{cap} = 0.95$.

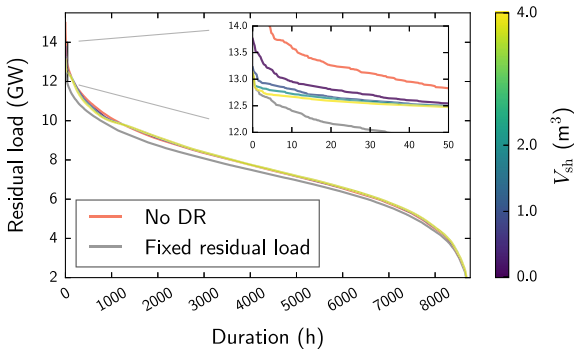

Fig. 7. Residual load duration diagrams for different storage tank sizes. The fixed residual load and load duration diagram without DR are presented in gray and red respectively.

Differences between different storage sizes are most clear in the region below 50 h duration. Here can be seen that increasing the storage capacity, decreases the peak load up to a level similar to the fixed residual peak load. The decrease of load at low operating hours is made up by an increased energy use at lower loads.

4.2. Required generation capacity

The residual peak load for all simulated cases is presented in Fig. 8. As almost no differences are observed with changing environmental impact of energy use weight, the peak load is presented with respect to the capacity limit. A lower capacity limit initially is accompanied by a strong decrease in residual peak load. However, when the capacity limit is decreased too much, the observed peak load increases slightly if a space heating storage tank is not present. When the peak load threshold is decreased the period the heat pump output must be lowered increases. When the available storage capacity is unable to supply heat to the building during this period, the heat pump will supply it to guarantee thermal comfort. Furthermore, due to the complex dynamics of the hot water storage charging and the non-linearity of the heat pump COP, there is a model mismatch between the controller and the actual storage tank and heat pump or the emulator. When the settings become more critical, the OCP will generate solutions which are closer to the boundaries of acceptable operation. A small mismatch between control and emulator could then also lead to the observed increase.

Without a space heating storage tank, the minimum residual peak load is around 0.61 GW higher than the fixed residual load peak of 13.12 GW. This minimum is obtained with a control setting

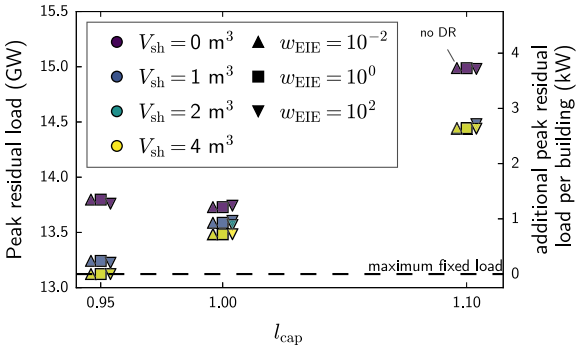

Fig. 8. Variation of the peak residual load with variation of the control parameters and the space heating storage size. The peak load for the total system is presented on the left axis. On the right axis, the increase in peak load above the fixed peak load divided by the number of buildings is presented. For clarity the markers with different environmental impact of energy use weight are slightly shifted left or right.

$l_{cap} = 1.00$. On the right scale of Fig. 8, the additional peak load, above the fixed residual load peak, divided by the number of buildings is displayed. This scale thus assigns the additional peak load to the system causing it. Without a space heating storage tank a decrease from 3.7 kW without DR to 1.2 kW with DR is observed.

When a space heating storage tank is added to the building heating system, the residual peak load can be further decreased. When a 2 m^3 or larger space heating storage tank is used, the peak load is decreased to the maximum fixed residual load. Nevertheless, the decrease in peak load when comparing the cases without storage and with 1 m^3 space heating storage tank is around 0.50 GW, while the decrease when comparing the 1 m^3 and 2 m^3 cases is only 0.11 GW. This suggests a trade-off can be made between installing larger space heating storage tanks or increasing the peak generating capacity.

The maximum effect of adding a hot water storage tank is obtained with a 1 m^3 tank. In this case, the maximum residual load decreases from 13.73 GW (without space heating storage tank) to 13.23 GW (with a 1 m^3 space heating storage tank in 500,000 buildings) or around 1 kW/m^3 storage tank.

4.3. Energy use

In Fig. 9a the total residual energy use is shown. In Fig. 9b and c the residual energy is split into the part generated by base load plants and by peak load plants respectively. As the environmental impact of energy use weight control setting is increased, the amount of energy generated by peak load power plants drops from around 2000 kW h to around 900 kW h per building. The amount of energy generated by base load power plants rises from around 2900 kW h to around 4200 kW h per building. Due to the lower impact assigned to base load electricity generation the control attempts to shift energy generation from peak to base load plants. Accordingly, the residual energy use rises by around 200 kW h per building on a total yearly electricity use of around 4850 kW h in the case of no DR. This corresponds to a nationwide increase in electricity use of around 100 GW h. To maintain thermal comfort for the building inhabitants, thermal energy is stored in either the floor heating system or the hot water storage tank. Both imply energy losses counteracting the shift from peak load generation to base load generation and increasing the total energy requirement.

The addition of a storage tank always decreases the energy generated by peak load plants by 60 kW h to 300 kW h per building depending on the energy control setting and storage size. A larger storage size always results in less energy generated by peak load plants. When the space heating buffer is added to the system, the residual energy use increases due to the additional heat losses from the storage tank. However, as the storage tank size increases the residual energy use is lowered. With increasing volume the surface area of the storage tank, governing the heat losses, only increases with a power of around 2/3 while more load shifting flexibility is offered. The increase in residual energy use with rising space heating storage tank volume is largest with a low environmental impact of energy use weight (w_{EIE}). When this setting is low, the control system attempts to minimize the local electricity cost. As the electricity price is not correlated with the source of electricity or the availability of renewable sources, this results in an overall increase in energy use by storing energy when the price is low. With a high energy control setting, the control attempts to reduce the energy generated by peak load plants and replaces it with energy produced by base load plants.

When lowering the capacity limit both energy use from base load plants and peak load plants increase slightly in all cases. When the capacity is tightly constrained, the control must decrease the peak load at the expense of energy use.

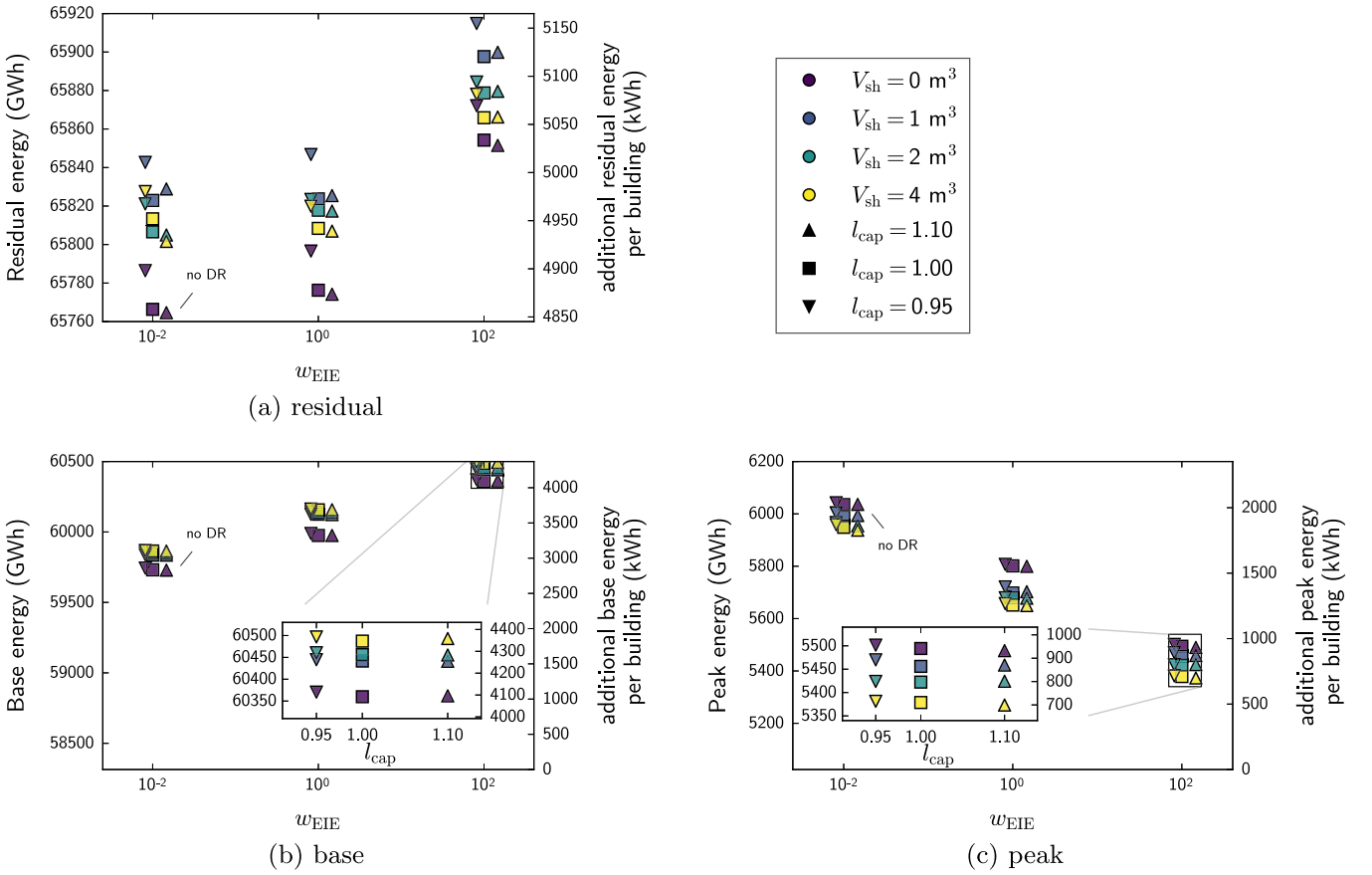

Fig. 9. Variation of the residual energy use with variation of the control parameters and the space heating storage size. The total residual energy is shown in (a), energy generated by base load plants is shown in (b), energy generated by peak load plants is shown in (c). The energy use for the total system is presented on the left axis. On the right axis, the increase in energy use above the fixed energy use divided by the number of buildings is presented. For clarity the markers with different capacity limit settings are slightly shifted left or right.

4.4. Consumer cost

Fig. 10 presents the cost of space heating and domestic hot water production as seen by the consumer as a function of the environmental impact of energy use weight control setting. The general view of this figure is similar to the residual energy use (Fig. 9a). In the presented case, the difference between day time and night time electricity prices is too small for a significant shift in energy use to the night to occur. As in the presented case no curtailing occurs the figures are alike.

When the consumer does not participate in DR, the local costs are minimum. When participating in a demand response program the costs carried by the consumer can increase by up to 70 EUR per year. The largest increase is obtained when the energy control setting is maximum and capacity control setting is minimum. In this case the local cost only marginally affects the OCP objective function. Adding a storage tank to the system increases heat losses and thus will increase energy use. Even if the consumer does not participate in DR, the additional flexibility provided by the hot water storage tank cannot induce a reduction in costs. In the presented boundary conditions, the variation in electricity price is too small. Furthermore, the variation in ambient temperature most often results in a low heat pump COP during the night, when electricity prices are low. This further discourages shifting energy use to the low price periods.

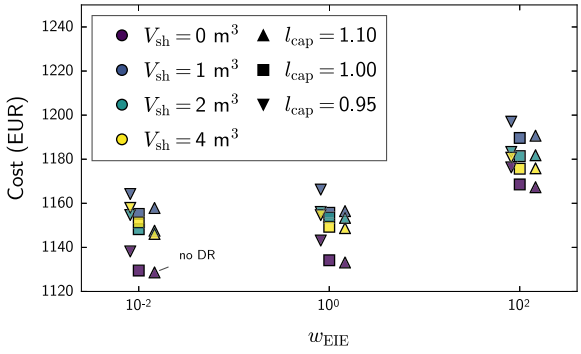

Fig. 10. Variation of the local operational costs per building with variation of the control parameters and the space heating storage size. For clarity the markers with different capacity limit control settings are slightly shifted left or right.

From this can be concluded that if DR is desired by a grid operator, aggregator or other party involved, heat pump owners should be encouraged to participate by compensating them for their additional costs. The services provided by consumers can be remunerated through adapted energy prices [29] or by granting a discount to users who participate in DR programs or a penalty for those that do not.

When Figs. 8 and 10 are combined an interesting observation is made. When consumers switch from not participating in DR to applying a control strategy which limits the total residual load ($l_{cap} = 1.10 \rightarrow l_{cap} = 1.00$) the increase in consumer costs never exceeds 2 EUR per year. However, this change in setting causes the maximum residual load to decrease by 2.5 kW per building from 14.99 GW to 13.74 GW, a 1.25 GW decrease. When a power plant lifetime is assumed 25 years, this results in a capacity cost of less than 25 EUR/kW which is very small compared to values for open cycle gas turbine power plants found in the literature which lie between 200 EUR/kW and 400 EUR/kW [39].

Adding a 2 m^3 space heating storage tank and lowering the capacity control setting to 0.95 further lowers the maximum load from 13.74 GW to the fixed residual load. However, the consumer costs are increased with up to 26 EUR per year compared to the case without DR and storage tank. When comparing this value with the costs for installing additional generation capacity, the investment in the storage tank will probably not be favorable.

4.5. Overall merit of different control settings

When discussing the merit of the presented control strategies and their resulting energy use and required generating capacity, several viewpoints are possible. In a financial viewpoint, costs can be assigned to the generation of electricity by different plants and to the construction of generating plants. The resulting cost of electricity generation can then be compared with the total investment cost required for the storage tanks and heat pumps. On the other hand, emissions from the construction and operation of all subsystems could be calculated through a life cycle analysis (LCA), resulting in an environmental comparison. In this paper no specific viewpoint is adopted although, in the presented case study, the controller uses environmental impact costs derived from the Ecoinvent LCA database.

5. Conclusions

The use of heat pumps for residential space heating can reduce greenhouse gas emissions and increase the energy efficiency of buildings. If large numbers of heat pumps are introduced in an electricity system, demand response can be employed to avoid adverse effects of the accompanying decrease in load diversity.

In this paper, a multi-objective model predictive control strategy for space heating and domestic hot water production using a heat pump and thermal energy storage in a residential demand response context is described. Depending on two control parameters, the controller accounts for consumer costs, impact of energy use in the national electricity system and impact of required additional power generating capacity. Results are presented for a case study inspired by the Belgian electricity system with an increase in renewable based generating capacity and the switch of 500,000 buildings to heating with heat pumps.

In contrast to papers found in the literature, this study employs a detailed emulator model for the hot water storage tank and a heat pump performance map to account for the temperature and modulation dependency of the heat pump output. In addition, the heating control system employs an integrated optimization of the electricity generation park and the demand side.

Through demand response with a controller which limits the total residual load, a significant reduction in required generation capacity is possible with only a minor increase in consumer costs. The addition of a storage tank lowers the required generation capacity even further but consumer cost also increases.

By increasing the importance of the environmental impact of the generated electricity, the amount of energy generated by peak load power plants is reduced significantly independently of the peak load reduction. Adding a hot water storage buffer for space heating further reduces load peaks and energy generated by peak load power plants, however the decrease is less striking.

When further adjusting the control settings and adding a space heating hot water storage tank, the required peak load capacity can be reduced to the required capacity without heat pumps. The energy generated by peak load power plants can be lowered by up to 11% together with only a slightly larger increase in energy generated by base load plants. However, these control settings cause the operational costs seen by the consumer to increase substantially. If this reduction in required capacity or peak energy use is desired by the grid operator or other stakeholders, they can consider encouraging heat pump owners to participate in demand response programs with similar control strategies and remunerating them for their additional expenses.

Appendix A. Optimal control problem

A.1. Building

The differential equations governing the building states can be written as:

$$C_{\mathrm{in}}\frac{\mathrm{d}T_{\mathrm{in}}}{\mathrm{d}t}=\frac{T_{\mathrm{amb}}-T_{\mathrm{in}}}{R_{\mathrm{ve}}}+\frac{T_{\mathrm{wi}}-T_{\mathrm{in}}}{R_{\mathrm{wi}}}+\frac{T_{\mathrm{we}}-T_{\mathrm{in}}}{R_{\mathrm{w1}}}+\frac{T_{\mathrm{fl}}-T_{\mathrm{in}}}{R_{\mathrm{f1}}}+\dot{Q}_{\mathrm{in}} \quad (A.1)$$

$$C_{\mathrm{wi}}\frac{\mathrm{d}T_{\mathrm{wi}}}{\mathrm{d}t}=\frac{T_{\mathrm{in}}-T_{\mathrm{wi}}}{R_{\mathrm{wi}}}+\dot{Q}_{\mathrm{wi}} \quad (A.2)$$

$$C_{\mathrm{we}}\frac{\mathrm{d}T_{\mathrm{we}}}{\mathrm{d}t}=\frac{T_{\mathrm{in}}-T_{\mathrm{we}}}{R_{\mathrm{w1}}}+\frac{T_{\mathrm{amb}}-T_{\mathrm{we}}}{R_{\mathrm{w2}}}+\dot{Q}_{\mathrm{we}} \quad (A.3)$$

$$C_{\mathrm{fl}}\frac{\mathrm{d}T_{\mathrm{fl}}}{\mathrm{d}t}=\frac{T_{\mathrm{in}}-T_{\mathrm{fl}}}{R_{\mathrm{f1}}}+\frac{T_{\mathrm{tr}}-T_{\mathrm{fl}}}{R_{\mathrm{f2}}}+\dot{Q}_{\mathrm{fl}} \quad (A.4)$$

$$C_{\mathrm{tr}}\frac{\mathrm{d}T_{\mathrm{tr}}}{\mathrm{d}t}=\frac{T_{\mathrm{fl}}-T_{\mathrm{tr}}}{R_{\mathrm{f2}}}+\frac{T_{\mathrm{gnd}}-T_{\mathrm{tr}}}{R_{\mathrm{tr}}}+\frac{T_{\mathrm{sh}}-T_{\mathrm{tr}}}{R_{\mathrm{sh}}}+\frac{T_{\mathrm{dw}}-T_{\mathrm{tr}}}{R_{\mathrm{dw}}}+\dot{Q}_{\mathrm{hp,loss}} \quad (A.5)$$

In the optimal control problem, heat losses from the heat pump to the technical room are neglected. The equations are discretized to:

$$C_{\mathrm{in}}\frac{T_{\mathrm{in}}^{i+1}-T_{\mathrm{in}}^{i}}{\Delta t}=\frac{T_{\mathrm{amb}}^{i}+T_{\mathrm{amb}}^{i+1}-T_{\mathrm{in}}^{i}-T_{\mathrm{in}}^{i}}{2R_{\mathrm{ve}}}+\frac{T_{\mathrm{wi}}^{i}+T_{\mathrm{wi}}^{i+1}-T_{\mathrm{in}}^{i}-T_{\mathrm{in}}^{i+1}}{2R_{\mathrm{wi}}}+\frac{T_{\mathrm{we}}^{i}+T_{\mathrm{we}}^{i+1}-T_{\mathrm{in}}^{i}-T_{\mathrm{in}}^{i+1}}{2R_{\mathrm{w1}}}+\frac{T_{\mathrm{fl}}^{i}+T_{\mathrm{fl}}^{i+1}-T_{\mathrm{in}}^{i}-T_{\mathrm{in}}^{i+1}}{2R_{\mathrm{f1}}}+\dot{Q}_{\mathrm{in}} \quad (A.6)$$

$$C_{\mathrm{wi}}\frac{T_{\mathrm{wi}}^{i+1}-T_{\mathrm{wi}}^{i}}{\Delta t}=\frac{T_{\mathrm{in}}^{i}+T_{\mathrm{in}}^{i+1}-T_{\mathrm{wi}}^{i}-T_{\mathrm{wi}}^{i+1}}{2R_{\mathrm{wi}}}+\dot{Q}_{\mathrm{wi}} \quad (A.7)$$

$$C_{\mathrm{we}}\frac{T_{\mathrm{we}}^{i+1}-T_{\mathrm{we}}^{i}}{\Delta t}=\frac{T_{\mathrm{in}}^{i}+T_{\mathrm{in}}^{i+1}-T_{\mathrm{we}}^{i}-T_{\mathrm{we}}^{i+1}}{2R_{\mathrm{w1}}}+\frac{T_{\mathrm{amb}}^{i}+T_{\mathrm{amb}}^{i+1}-T_{\mathrm{we}}^{i}-T_{\mathrm{we}}^{i+1}}{2R_{\mathrm{w2}}}+\dot{Q}_{\mathrm{we}} \quad (A.8)$$

$$C_{\mathrm{fl}}\frac{T_{\mathrm{fl}}^{i+1}-T_{\mathrm{fl}}^{i}}{\Delta t}=\frac{T_{\mathrm{in}}^{i}+T_{\mathrm{in}}^{i+1}-T_{\mathrm{fl}}^{i}-T_{\mathrm{fl}}^{i+1}}{2R_{\mathrm{f1}}}+\frac{T_{\mathrm{tr}}^{i}+T_{\mathrm{tr}}^{i+1}-T_{\mathrm{fl}}^{i}-T_{\mathrm{fl}}^{i+1}}{2R_{\mathrm{f2}}}+\dot{Q}_{\mathrm{fl}} \quad (A.9)$$

$$C_{\mathrm{tr}}\frac{T_{\mathrm{tr}}^{i+1}-T_{\mathrm{tr}}^{i}}{\Delta t}=\frac{T_{\mathrm{fl}}^{i}+T_{\mathrm{fl}}^{i+1}-T_{\mathrm{tr}}^{i}-T_{\mathrm{tr}}^{i+1}}{2R_{\mathrm{f2}}}+\frac{T_{\mathrm{gnd}}^{i}+T_{\mathrm{gnd}}^{i+1}-T_{\mathrm{tr}}^{i}-T_{\mathrm{tr}}^{i+1}}{2R_{\mathrm{tr}}}+\frac{T_{\mathrm{sh}}^{i}+T_{\mathrm{sh}}^{i+1}-T_{\mathrm{tr}}^{i}-T_{\mathrm{tr}}^{i+1}}{2R_{\mathrm{sh}}}+\frac{T_{\mathrm{dw}}^{i}+T_{\mathrm{dw}}^{i+1}-T_{\mathrm{tr}}^{i}-T_{\mathrm{tr}}^{i+1}}{2R_{\mathrm{dw}}} \quad (A.10)$$

Heat flows to the different components as a result of solar and internal gains are computed as:

$$\begin{aligned}\dot{Q}_{\mathrm{wi}}&=f_{\mathrm{sol,wi}}S^{i}\frac{1}{2}\left(\dot{Q}_{\mathrm{sol}}^{i}+\dot{Q}_{\mathrm{sol}}^{i+1}\right)\\ \dot{Q}_{\mathrm{in}}&=f_{\mathrm{sol,in}}S^{i}\frac{1}{2}\left(\dot{Q}_{\mathrm{sol}}^{i}+\dot{Q}_{\mathrm{sol}}^{i+1}\right)+\dot{Q}_{\mathrm{gain}}^{i}\\ \dot{Q}_{\mathrm{we}}&=f_{\mathrm{sol,we}}S^{i}\frac{1}{2}\left(\dot{Q}_{\mathrm{sol}}^{i}+\dot{Q}_{\mathrm{sol}}^{i+1}\right)\\ \dot{Q}_{\mathrm{fl}}&=f_{\mathrm{sol,fl}}S^{i}\frac{1}{2}\left(\dot{Q}_{\mathrm{sol}}^{i}+\dot{Q}_{\mathrm{sol}}^{i+1}\right)+\dot{Q}_{\mathrm{sh}}^{i}\end{aligned} \quad (A.11)$$

The building operative temperature is linearized according to [40]:

$$T^i_{op} = 0.4\ T^i_{in} + 0.6\ (0.3\ T^i_{we} + 0.3\ T^i_{wi} + 0.4\ T^i_{fl}) \quad (A.12)$$

Thermal discomfort costs are computed as:

$$\text{discomfort costs}^i = p_d \max(0, T^i_{op,max} - T^i_{op}) + p_d \max(0, T^i_{op} - T^i_{op,max}) \quad (A.13)$$

A.2. Heating system

The heat pump can supply heat for space heating or for domestic hot water production:

$$\dot{Q}^i_{hp,lt} = \dot{Q}^i_{hp,lt,sh} + \dot{Q}^i_{hp,lt,dw} \quad (A.14)$$

$$\dot{Q}^i_{hp,mt} = \dot{Q}^i_{hp,mt,sh} + \dot{Q}^i_{hp,mt,dw} \quad (A.15)$$

$$\dot{Q}^i_{hp,ht} = \dot{Q}^i_{hp,ht,sh} + \dot{Q}^i_{hp,ht,dw} \quad (A.16)$$

The variation in heat pump efficiency with ambient temperature, leaving water temperature and compressor modulation is accounted for as:

$$P_{hp} = P_{hp,lt} + P_{hp,mt} + P_{hp,ht} \quad (A.17)$$

$$P_{hp,lt} \geqslant \zeta_{l,lt}(T_{amb})\dot{Q}_{hp,lt} + \zeta_{q,lt}(T_{amb})\dot{Q}^2_{hp,lt} \quad (A.18)$$

$$P_{hp,mt} \geqslant \zeta_{l,mt}(T_{amb})\dot{Q}_{hp,mt} + \zeta_{q,mt}(T_{amb})\dot{Q}^2_{hp,mt} \quad (A.19)$$

$$P_{hp,ht} \geqslant \zeta_{l,ht}(T_{amb})\dot{Q}_{hp,ht} + \zeta_{q,ht}(T_{amb})\dot{Q}^2_{hp,ht} \quad (A.20)$$

The auxiliary heater efficiency is assumed to be 1:

$$P^i_{aux} = \dot{Q}^i_{aux} \quad (A.21)$$

The space heating storage state is computed from:

$$C_{sh}\frac{T^{i+1}_{sh} - T^i_{sh}}{\Delta t} = \frac{T^i_{tr} + T^{i+1}_{tr} - T^i_{sh} - T^{i+1}_{sh}}{2R_{sh}} + \dot{Q}^i_{hp,lt,sh} + \dot{Q}^i_{hp,mt,sh} + \dot{Q}^i_{hp,ht,sh} - \dot{Q}^i_{em} \quad (A.22)$$

With additional constraints:

$$\dot{Q}^i_{hp,sh} \leqslant \rho c \dot{V}^{max}_{hp}(T_{hp} - T_{em,ret}) \quad (A.23)$$

$$\dot{Q}^i_{em} \leqslant \varepsilon^{nom}\rho c \dot{V}^{max}_{em}\left(T_{hp} - T^i_{fl}\right) \quad (A.24)$$

$$T^i_{sh} \leqslant T_{hp} \quad (A.25)$$

$$T^i_{sh} \geqslant T_{em,ret} \quad (A.26)$$

The domestic hot water storage tank state is computed from:

$$C_{dw,lt}\frac{T^{i+1}_{dw,lt} - T^i_{dw,lt}}{\Delta t} = \frac{T^i_{tr} + T^{i+1}_{tr} - T^i_{dw,lt} - T^{i+1}_{dw,lt}}{2R_{dw}} + \dot{Q}^i_{hp,lt,dw} - \dot{Q}^i_{dw,lt} \quad (A.27)$$

$$C_{dw,mt}\frac{T^{i+1}_{dw,mt} - T^i_{dw,mt}}{\Delta t} = -\frac{T^i_{dw,mt} - T^{i+1}_{dw,mt}}{2R_{dw}} + \dot{Q}^i_{hp,mt,dw} - \dot{Q}^i_{dw,mt} \quad (A.28)$$

$$C_{dw,ht}\frac{T^{i+1}_{dw,ht} - T^i_{dw,ht}}{\Delta t} = -\frac{T^i_{dw,ht} - T^{i+1}_{dw,ht}}{2R_{dw}} + \dot{Q}^i_{hp,ht,dw} - \dot{Q}^i_{dw,ht} \quad (A.29)$$

$$C_{dw,vht}\frac{T^{i+1}_{dw,vht} - T^i_{dw,vht}}{\Delta t} = -\frac{T^i_{dw,vht} - T^{i+1}_{dw,vht}}{2R_{dw}} + \dot{Q}^i_{aux} - \dot{Q}^i_{dw,vht} \quad (A.30)$$

With additional constraints:

$$T^i_{dw} = T^i_{dw,lt} + T^i_{dw,mt} + T^i_{dw,ht} + T^i_{dw,vht} \quad (A.31)$$

$$\dot{Q}^i_{dw} = \dot{Q}^i_{dw,lt} + \dot{Q}^i_{dw,mt} + \dot{Q}^i_{dw,ht} + \dot{Q}^i_{dw,vht} \quad (A.32)$$

$$\dot{Q}^i_{dw} = \rho c \dot{V}^i_{dw}(T_{dw,dem} - T_{mains}) \quad (A.33)$$

$$\dot{Q}^i_{hp,dw,lt} \leqslant \rho c \dot{V}^{max}_{hp}\left(T_{hp,lt} - T^i_{dw,lt}\right) \quad (A.34)$$

$$\dot{Q}^i_{hp,dw,lt} \leqslant \rho c \dot{V}^{max}_{hp}\left(T_{hp,lt} - T^{i+1}_{dw,lt}\right) \quad (A.35)$$

$$T^i_{dw,lt} \leqslant T_{hp,lt} \quad (A.36)$$

$$\dot{Q}^i_{hp,dw,mt} \leqslant \rho c \dot{V}^{max}_{hp}\left(T_{hp,mt} - T_{hp,lt} - T^i_{dw,mt}\right) \quad (A.37)$$

$$\dot{Q}^i_{hp,dw,mt} \leqslant \rho c \dot{V}^{max}_{hp}\left(T_{hp,mt} - T_{hp,lt} - T^{i+1}_{dw,mt}\right) \quad (A.38)$$

$$T^i_{dw,mt} \leqslant T_{hp,mt} - T_{hp,lt} \quad (A.39)$$

$$\dot{Q}^i_{hp,dw,ht} \leqslant \rho c \dot{V}^{max}_{hp}\left(T_{hp,ht} - T_{hp,mt} - T^i_{dw,ht}\right) \quad (A.40)$$

$$\dot{Q}^i_{hp,dw,ht} \leqslant \rho c \dot{V}^{max}_{hp}\left(T_{hp,ht} - T_{hp,mt} - T^{i+1}_{dw,ht}\right) \quad (A.41)$$

$$T^i_{dw,ht} \leqslant T_{hp,ht} - T_{hp,mt} \quad (A.42)$$

$$T^i_{dw,vht} \leqslant T^{i,max}_{dw} - T_{hp,ht} \quad (A.43)$$

$$T^i_{dw} \geqslant T^{i,min}_{dw} \quad (A.44)$$

A.3. Electricity generation

Supply and demand of electricity must be equal at all times. With N the number of buildings this results in:

$$NP^i_{hp} + NP^i_{aux} + P^i_{fixed} = P^i_{wind} + P^i_{pv} + P^i_{base} + P^i_{peak} \quad (A.45)$$

Renewables and base load generation have a limited capacity, for the renewables the maximum power is time dependent:

$$P^i_{wind} \leqslant P^{i,max}_{wind} \quad (A.46)$$

$$P^i_{pv} \leqslant P^{i,max}_{pv} \quad (A.47)$$

$$P^i_{base} \leqslant P^{max}_{base} \quad (A.48)$$

Base load generation has a limited ramping rate:

$$\frac{P^i_{base} - P^{i+1}_{base}}{\Delta t} \leqslant P^{max\ ramp}_{base}$$
$$\frac{P^i_{base} - P^{i+1}_{base}}{\Delta t} \geqslant -P^{max\ ramp}_{base} \quad (A.49)$$

The overload power is subject to:

$$P^i_{overload} \geqslant P^i_{residual} - l_{cap}P^{max}_{residual,fixed} \quad (A.50)$$

A.4. Objective

The multi-criterion objective is written as:

$$\text{minimize} \sum_{i=time} p^i_{el}(P^i_{hp} + P^i_{aux})\Delta t + \sum_{i=time}\sum_{j=sup} w_{EIE}\ p_{impact,j}P^i_j\Delta t + \sum_{i=time} p_{impact,\ cap}\left(P^i_{overload}\right)^2\Delta t + \sum_{i=time} \text{discomfort costs}^i \quad (A.51)$$

References

[1] IPCC. Climate Change 2014 synthesis report summary chapter for policymakers. Technical report, 2014.
[2] European Commission. Europe 2020: a strategy for smart, sustainable and inclusive growth. Technical report, 2010.

[3] European Commission. A policy framework for climate and energy in the period from 2020 to 2030. Technical report, 2014.
[4] Hewitt Neil J. Heat pumps and energy storage - the challenges of implementation. Appl Energy 2012;89(1):37–44.
[5] Waite Michael, Modi Vijay. Potential for increased wind-generated electricity utilization using heat pumps in urban areas. Appl Energy 2014;135:634–42.
[6] Zhang Ning, Lu Xi, McElroy Michael B, Nielsen Chris P, Chen Xinyu, Deng Yu, et al. Reducing curtailment of wind electricity in China by employing electric boilers for heat and pumped hydro for energy storage. Appl Energy 2016;184:987–94.
[7] Strbac Goran. Demand side management: benefits and challenges. Energy Policy 2008;36(12):4419–26.
[8] Vanhoudt D, Geysen D, Claessens B, Leemans F, Jespers L, Van Bael J. An actively controlled residential heat pump: Potential on peak shaving and maximization of self-consumption of renewable energy. Renew Energy 2014;63(0):531–43.
[9] Warren Peter. A review of demand-side management policy in the UK. Renew Sustain Energy Rev 2014;29:941–51.
[10] Cooper Samuel JG, Hammond Geoffrey P, McManus Marcelle C, Rogers John G. Impact on energy requirements and emissions of heat pumps and micro-cogenerators participating in demand side management. Appl Thermal Eng 2014;71(2):872–81.
[11] Arteconi Alessia, Patteeuw Dieter, Bruninx Kenneth, Delarue Erik, D'haeseleer William, Helsen Lieve. Active demand response with electric heating systems: impact of market penetration. Appl Energy 2016;177:636–48.
[12] Kreuder Lukas, Spataru Catalina. Assessing demand response with heat pumps for efficient grid operation in smart grids. Sustain Cities Soc 2015;19:136–43.
[13] Arteconi Alessia, Hewitt Neil J, Polonara Fabio. Domestic demand-side management (DSM): Role of heat pumps and thermal energy storage (TES) systems. Appl Therm Eng 2013;51(1–2):155–65.
[14] Patteeuw Dieter, Reynders Glenn, Bruninx Kenneth, Protopapadaki Christina, Delarue Erik, D'haeseleer William, Saelens Dirk, Helsen Lieve. CO_2-abatement cost of residential heat pumps with active demand response: demand- and supply-side effects. Appl Energy 2015;156:490–501.
[15] Hedegaard Karsten, Mathiesen Brian Vad, Lund Henrik, Heiselberg Per. Wind power integration using individual heat pumps Analysis of different heat storage options. Energy 2012;47(1):284–93.
[16] Baeten Brecht, Confrey Thomas, Pecue Sébastien, Rogiers Frederik, Helsen Lieve, Pecceu Sébastien, Rogiers Frederik, Helsen Lieve. A validated model for mixing and buoyancy in stratified hot water storage tanks for use in building energy simulations. Appl Energy 2016;172:217–29.
[17] Bianchini Gianni, Casini Marco, Vicino Antonio, Zarrilli Donato. Demand-response in building heating systems: a model predictive control approach. Appl Energy 2016;168:159–70.
[18] Zhao Yang, Lu Yuehong, Yan Chengchu, Wang Shengwei. MPC-based optimal scheduling of grid-connected low energy buildings with thermal energy storages. Energy Build 2015;86:415–26.
[19] Knudsen Michael Dahl, Petersen Steffen. Demand response potential of model predictive control of space heating based on price and carbon dioxide intensity signals. Energy Build 2016;125:196–204.
[20] Schibuola Luigi, Scarpa Massimiliano, Tambani Chiara. Demand response management by means of heat pumps controlled via real time pricing. Energy Build 2015;90:15–28.
[21] Dar Usman Ijaz, Sartori Igor, Georges Laurent, Novakovic Vojislav. Advanced control of heat pumps for improved flexibility of Net-ZEB towards the grid. Energy Build 2014;69:74–84.
[22] Vasallo Manuel Jesús, Bravo José Manuel. A MPC approach for optimal generation scheduling in CSP plants. Appl Energy 2016;165:357–70.
[23] Li Siwei, Joe Jaewan, Hu Jianjun, Karava Panagiota. System identification and model-predictive control of office buildings with integrated photovoltaic-thermal collectors, radiant floor heating and active thermal storage. Solar Energy 2015;113:139–57.
[24] Patteeuw Dieter, Bruninx Kenneth, Arteconi Alessia, Delarue Erik, D'haeseleer William, Helsen Lieve. Integrated modeling of active demand response with electric heating systems coupled to thermal energy storage systems. Appl Energy 2015;151:306–19.
[25] Modelica association <www.modelica.org>; 2016.
[26] Allgöwer Frank, Findeisen Rolf, Nagy Zoltan K. Nonlinear model predictive control. J Chin Inst Chem Eng 2004;35(3):299–315.
[27] Camacho Eduardo F, Bordons Carlos. Model predictive control. Springer-Verlag; 2007.
[28] Afram Abdul, Janabi-Sharifi Farrokh. Theory and applications of HVAC control systems: a review of model predictive control (MPC). Build Environ 2014;72:343–55.
[29] Patteeuw Dieter, Henze Gregor P, Helsen Lieve. Comparison of load shifting incentives for low-energy buildings with heat pumps to attain grid flexibility benefits. Appl Energy 2016;167:80–92.
[30] Cyx Wouter, Renders Nele, Van Holm Marlies, Verbeke Stijn. IEE TABULA - typology approach for building stock energy assessment. Technical report; 2011.
[31] Reynders Glenn. Quantifying the impact of building design on the potential of structural storage for active demand response in residential buildings, Ph.D. thesis. KU Leuven (Belgium); 2015.
[32] Reynders Glenn, Diriken Jan, Saelens Dirk. Quality of grey-box models and identified parameters as function of the accuracy of input and observation signals. Energy Build 2014;82(0):263–74.
[33] Vlieger Peter De, Kenhove Elisa Van, Janssens Arnold, Laverge Jelle. Dynamic thermal modeling of legionella pneumophila proliferation in domestic hot water systems. In: 14th Conference of international building performance simulation association. p. 1563–8.
[34] Baeten Brecht, Rogiers Frederik, Helsen Lieve. Energy cost reduction by optimal control of ideal sensible thermal energy storage in domestic space heating. In: Proceedings of the Eurotherm seminar 99 Conference, Lleida, Spain - Advances in thermal energy storage 01-045; 2014.
[35] Baeten Brecht, Rogiers Frederik, Patteeuw Dieter, Helsen Lieve. Comparison of optimal control formulations for stratified sensible thermal energy storage in space heating applications. In: Proceedings of the IEA-ECES-Greenstock conference, Bejing, China.
[36] Patteeuw Dieter, Helsen Lieve. Residential buildings with heat pumps, a verified bottom-up model for demand side management studies. In: 9th International conference on system simulation in buildings. p. 1–19.
[37] Elia NV. Grid data; 2013 <http://www.elia.be/en/grid-data>.
[38] Weidema BP, Bauer Ch, Hischier R, Mutel Ch, Nemecek T, Reinhard J, et al. The ecoinvent database: overview and methodology, data quality guideline for the ecoinvent database version 3. Technical report; 2013.
[39] European Commission. Energy Sources, Production Costs and Performance of Technologies for power generation, Heating and transport. Technical report; 2008.
[40] Owen Mark S, editor. ASHRAE handbook of fundamentals. ASHRAE; 2009.